Influence of soil and climate on root zone storage capacity

Euser, T; McMillan, H; Hrachowitz, M; Winsemius, H.C.; Savenije, HHG

DOI
10.1002/2015WR018115

Publication date
2016

Document Version
Final published version

Published in
Water Resources Research

AGU PUBLICATIONS

Water Resources Research

RESEARCH ARTICLE

10.1002/2015WR018115

Key Points:
- Plants develop their root systems to survive droughts
- Model root zone storage capacity (S_r) can be inferred from climate records
- Model experiment shows that S_r is stronger influenced by climate than by soil

Correspondence to:
T. de Boer-Euser,
t.euser@tudelft.nl

Citation:
Boer-Euser, T. ., H. K. McMillan, M. Hrachowitz, H. C. Winsemius, and H. H. G. Savenije (2016), Influence of soil and climate on root zone storage capacity, *Water Resour. Res.*, *52*, 2009–2024, doi:10.1002/2015WR018115.

Received 16 SEP 2015
Accepted 14 JAN 2016
Accepted article online 25 JAN 2016
Published online 16 MAR 2016

Influence of soil and climate on root zone storage capacity

Tanja de Boer-Euser[1], Hilary K. McMillan[2], Markus Hrachowitz[1], Hessel C. Winsemius[3], and Hubert H. G. Savenije[1]

[1]Water Resources Section, Faculty of Civil Engineering and Applied Geosciences, Delft University of Technology, Delft, Netherlands, [2]National Institute of Water and Atmospheric Research, Christchurch, New Zealand, [3]Deltares, Delft, Netherlands

Abstract Root zone storage capacity (S_r) is an important variable for hydrology and climate studies, as it strongly influences the hydrological functioning of a catchment and, via evaporation, the local climate. Despite its importance, it remains difficult to obtain a well-founded catchment representative estimate. This study tests the hypothesis that vegetation adapts its S_r to create a buffer large enough to sustain the plant during drought conditions of a certain critical strength (with a certain probability of exceedance). Following this method, S_r can be estimated from precipitation and evaporative demand data. The results of this "climate-based method" are compared with traditional estimates from soil data for 32 catchments in New Zealand. The results show that the differences between catchments in climate-derived catchment representative S_r values are larger than for soil-derived S_r values. Using a model experiment, we show that the climate-derived S_r can better reproduce hydrological regime signatures for humid catchments; for more arid catchments, the soil and climate methods perform similarly. This makes the climate-based S_r a valuable addition for increasing hydrological understanding and reducing hydrological model uncertainty.

1. Introduction

Root zone storage capacity (S_r) is an important hydrological descriptor, which strongly influences the hydrological functioning of a catchment. Root zone storage capacity can be understood as a volume of water per unit area within reach of plant roots for transpiration; outside this area of influence, water flows are largely controlled by gravity-induced gradients. In models, S_r is frequently used as a parameter representing catchment storage capacity in the dynamic part of the unsaturated zone. S_r controls water partitioning between evaporation and drainage, and thus the (long-term) water balance of a catchment [*Field et al.*, 1992; *Zhang et al.*, 2001]. Understanding the water balance and the associated dynamics of different storage components over time is essential to understand the hydrological functioning of a catchment, necessary for robust predictions of discharge and evaporation. Apart from hydrological purposes, accurate estimation of soil water storage and water fluxes (e.g., evaporation and discharge) is of critical importance for climate [e.g., *Kleidon and Heimann*, 2000; *Dirmeyer*, 2011; *Orth and Seneviratne*, 2014] and ecological models [e.g., *Liancourt et al.*, 2012; *Zelikova et al.*, 2015] as well.

Despite the importance of S_r, it is difficult to obtain well-founded catchment representative estimates. Although soil and plant root properties can be observed at the point scale, it remains problematic to integrate these measurements to the catchment scale due to their spatially heterogeneous character [e.g., *Crow et al.*, 2012]. Even if the soils were completely homogeneous, it is not necessarily clear how to map measured soil properties to model parameters, including S_r. Therefore, it is unknown whether point observations allow for an adequate representation of catchment representative S_r. Another common method to estimate S_r is by calibration, preferably using expert knowledge or additional data to guide or constrain the calibration [e.g., *Winsemius et al.*, 2008; *Gharari et al.*, 2014], which has the advantage that catchment representative S_r is directly estimated. On the other hand, even constrained calibration is subject to parameter sensitivity (i.e., equifinality) [*Beven*, 2006], making it again difficult to assess if the derived value is a plausible representation of the catchment representative S_r.

Following from the above, catchment understanding and flux modeling may be improved by further independent information on the amount of water which is (or can be) accessed by vegetation. The accessible

Table 1. Number of Selected Gauges for Combinations of Climate and Land Cover[a]

	Indigenous Forest	Grasses[b]	$\overline{P}$ (m yr^{-1})	$\overline{E_p}$ (m yr^{-1})	$\overline{Q}$ (m yr^{-1})
Warm-wet	1	6	1.8	0.9	1.2
Warm-dry	0	1	1.1	0.9	0.4
Cool-wet	14[c]	4	2.5	0.8	1.8
Cool-dry	0	6	1.0	0.8	0.3

[a]Warm: $\overline{T_{year}} > 12^\circ$C, cool: $\overline{T_{year}} < 12^\circ$C, dry: $\overline{P-E_p} < 500$ mm yr^{-1}), wet: $\overline{P-E_p} > 500$ mm yr^{-1} (this category contains areas classified as "wet" and as "extremely wet" in Figure 1).
[b]This category contains both pasture and tussock grasses.
[c]This category contains one catchment with shrub land cover.

water amount is not necessarily related to root depth, but rather to root density, i.e., the pore volume within the area of influence of the roots [*Schenk and Jackson*, 2002; *Gentine et al*., 2012; *Cassiani et al*., 2015; *Tron et al*., 2015; *Brunner et al*., 2015]. To ensure long-term survival, vegetation adapts to its environment [*Eagleson*, 1982; *Canadell et al*., 1996; *Sampson and Allen*, 1999; *Troch et al*., 2009]. Vegetation attempts to balance the resources invested in above surface growth with the resources necessary to create a root zone storage capacity large enough to buffer hydrological variability and to provide sufficient water for survival. This is an example of the widely acknowledged interaction between climate and vegetation [*Milly*, 1994; *Rodriguez-Iturbe*, 2000; *Schymanski et al*., 2008]. It is likely that the required S_r is strongly dependent on climate [*Kleidon and Heimann*, 1998; *Donohue et al*., 2012; *Gentine et al*., 2012], i.e., precipitation and evaporative demand, but that the dependence on soil type is much weaker: in a specific climate, vegetation needs a certain amount of water, irrespective of the soil type it is growing on. Two similar plants in the same climate, but on different soil type, might develop a different root structure, but they will require the same amount of buffer capacity to survive [cf. *Camporese et al*., 2015].

Climatic variability is characterized by higher frequency temporal dynamics than the formation process of soils. In turn, it is plausible that the medium-term dynamics of root growth have the same time scale as climatic variability [e.g., *Sivandran and Bras*, 2013]; thus, when S_r depends on climate rather than on soil, this would mean that S_r should be dynamic at time scales of climatic variability. This supports the results of various hydrological modeling studies that have also shown the need for a variable reflecting medium-term dynamics [e.g., *Wagener et al*., 2003; *Fenicia et al*., 2009]. *Beekman et al*. [2014] showed that a model based on soil data underestimates the evaporation of a forest on sandy soil and overestimates the evaporation of crops on clay soil during a very dry summer in Netherlands. Although the modeled evaporation above the forest was almost zero, the vegetation survived the drought. Hence, we may assume that the vegetation did develop a root system which could adapt to the climatic variability and thus created a buffer large enough to bridge the dry summer [cf. *Vico et al*., 2015], even on the sandy soil. This follows the line of argument set by *Gimbel et al*. [2015], who concluded that medium-term to long-term climatic conditions of an area were more important than short-term antecedent soil moisture for the system behavior under drought conditions.

Kleidon and Heimann [1998] showed that root depth is strongly related to climate, especially to the difference in precipitation and potential evaporation. Following on this, *Gao et al*. [2014] recently successfully demonstrated for 400 catchments in the U.S. that catchment representative root zone storage capacities estimated from climate are strongly correlated with estimates derived from the calibration of a hydrological model. These studies indicate that climate information contains at least a certain level of information on root zone dynamics and thus on the influence of vegetation on the partitioning of water fluxes. Based on the results of *Gao et al*. [2014] and following the arguments above, we here extend the work of *Gao et al*. [2014] and test the hypothesis that climate is a more suitable estimator for the catchment-scale root zone storage capacity S_r than observation inferred soil characteristics.

2. Study Areas

New Zealand lies on a fault line, and therefore, has a high mountain range (the Southern Alps) spanning the country in a north-south direction. This mountain range, combined with prevailing westerly winds, causes a

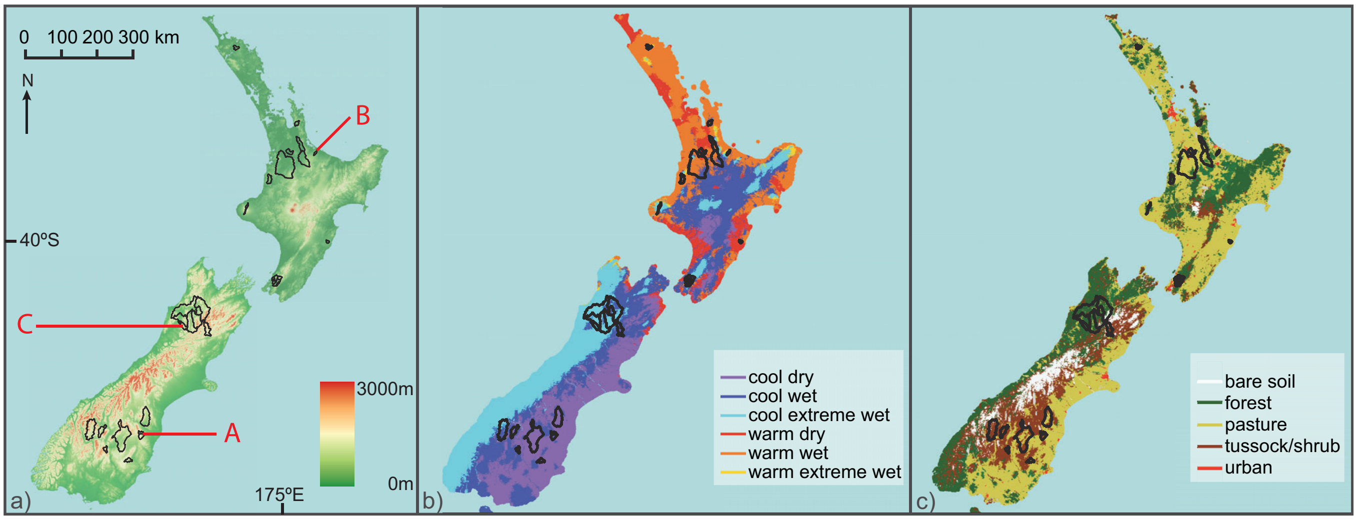

Figure 1. Thirty-two catchments with different backgrounds: (a) elevation (A, B and C indicate the catchments used in Figures 8 and 11); (b) climate; and (c) land cover.

strong climatic gradient over a distance of 200 km, with yearly precipitation ranging from less than 0.6 m yr^{-1} on the eastern (lee) side to more than 10 m yr^{-1} on the western (windward) side. Mean annual temperatures also vary across the country from 16°C in the north to 10°C in the south [*NIWA*, 2015]. Before human colonization, the predominant land cover was indigenous forest; this forest is now confined to the mountain ranges, with pasture and crop land dominating elsewhere.

Thirty-two New Zealand catchments were analyzed in this study (Table 1 and Figure 1); they were mainly selected for variability in size (fourth to seventh Strahler-order streams), climate, and land cover. An example of differences in climate is shown in Figure 2a: for each climate category in Table 1, the average monthly precipitation and potential evaporation are shown. The catchments with more than 20 years of discharge data were selected from the set used by *Booker and Woods* [2014], containing catchments with limited human influence. Catchments with lake or glacial influence were not selected to prevent the effect of inter annual storage changes. Finally, some nested catchments were specifically selected; these were used to

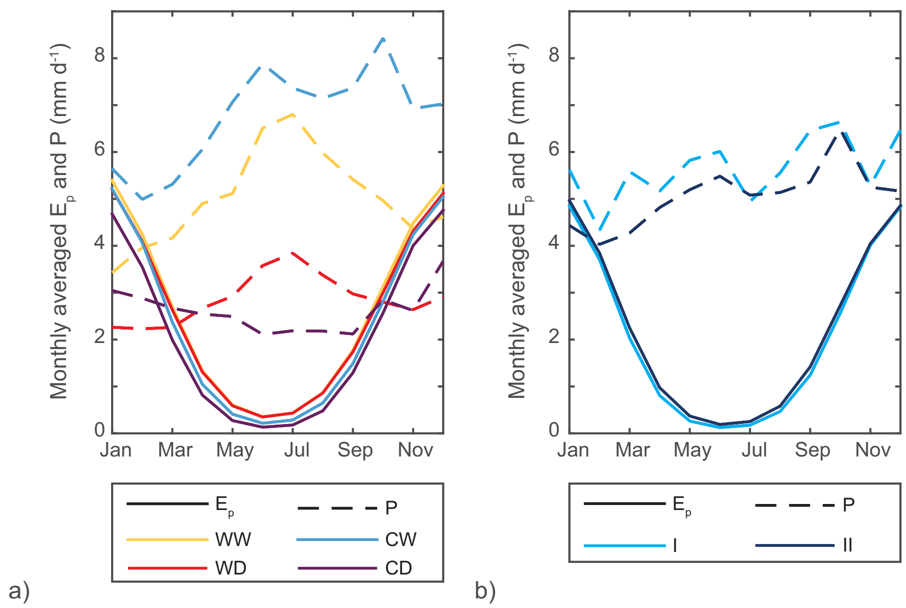

Figure 2. Monthly averaged precipitation (*P*; dashed lines) and potential evaporation (E_p; solid lines); (a) averaged values for each climate category in Table 1 (WW = Warm Wet, WD = Warm Dry, CW = Cool Wet, and CD = Cool Dry); (b) values for catchments I and II in Figure 7.

Table 2. Characteristics of Subset of Catchments[a]

	A	B	C
Aridity index ($\overline{E_p}/\overline{P}$)	0.67	0.40	0.32
Long-term averaged runoff coefficient	0.42	0.48	0.84
Mean annual precipitation (m yr^{-1})	1.1	2.4	2.6
Mean annual pot. evaporation (m yr^{-1})	0.74	0.97	0.82
Seasonality precipitation	0.16	0.15	0.11
Seasonality pot. evaporation	0.72	0.61	0.69
Number of months between peak P and E_p	0	7	3
Dominant climate	Cool-dry	Warm-wet	Cool-extremely wet
Dominant land cover	Pasture	Pasture	Forest
Derived $S_{r,soil}$ (m)	0.16	0.15	0.17
Derived $S_{r,clm}$ (m)	0.14	0.31	0.02

[a]This subset of catchments was used for more specific analyses: hydrograph analysis and sensitivity analysis.

investigate several possible methods to disaggregate the climate-derived, catchment representative S_r to nested subcatchments.

All selected catchments were used for the overall comparison between climate-derived and soil-derived S_r values. Additionally, some analyses were carried out for a subset of catchments only. Using a selection of catchments makes it possible to point out some effects in more detail. The catchments in this subset are Otekaieke at Stockbridge (A), Raparapahoe at drop structure (B), and Inangahua at Blacks point (C). The catchments vary in aridity, land cover, and size, see Table 2 for more details and Figure 1 for locations.

Daily discharge data were available from flow gauges; daily precipitation and potential evaporation data were available from the Virtual Climate Station Network (VCSN) [*Tait et al.*, 2006, 2012], which contains interpolated data at a 0.05° grid at daily time steps. The VCSN is comprised from national rain gauge data; mountainous areas have a lower gauge density, leading to less reliable estimates at these locations. Potential evaporation was calculated with the Priestley Taylor method [*Priestley and Taylor*, 1972]. Catchment average precipitation and potential evaporation estimates were used from 1972 to 2012. The VCSN precipitation data were corrected for spatial bias, using an analysis of the long-term water balance: mean annual modeled runoff was compared with observed mean annual runoff and errors were assumed to be mainly caused by inaccuracies in precipitation measurements [*Woods et al.*, 2006]. The available discharge data varied per catchment, both in length and in period; however, for each catchment, at least 20 complete years were available.

3. Methods

3.1. Comparison of Soil-Derived and Climate-Derived Root Zone Storage Capacity

Soil and climate-derived S_r values ($S_{r,soil}$ and $S_{r,clm}$, respectively) were calculated for a variety of catchments (description in section 3.2). The soil and climate methods were compared based on these derived values and based on model results with these derived values.

3.1.1. Comparison Based On Derived S_r Values

Comparison of the soil-derived and climate-derived S_r values was based on spatial patterns and scatterplots. Catchment representative S_r values were compared based on their location in New Zealand. In addition, they were compared with a scatterplot, in which the catchment average runoff coefficient was used as an explanatory factor.

3.1.2. Comparison Based On Model Results

Soil-derived and climate-derived S_r values are based on different methods, but the values should be similar when assuming that they both represent the catchment representative root zone storage capacity. Although, it may not be possible to determine which S_r estimate is closer to the true catchment value, we can test which estimate is more suitable for a modeling concept of root zone storage capacity. This second comparison is made using the hydrological model TopNet, which is run with each S_r estimate in turn. The modeled and observed discharges were compared using hydrological signatures [e.g., *Euser et al.*, 2013; *Winsemius et al.*, 2009; *McMillan et al.*, 2013].

TopNet is a distributed conceptual model covering all third-order subcatchments in New Zealand. The national version is not calibrated, but parameters are estimated for each third-order subcatchment from

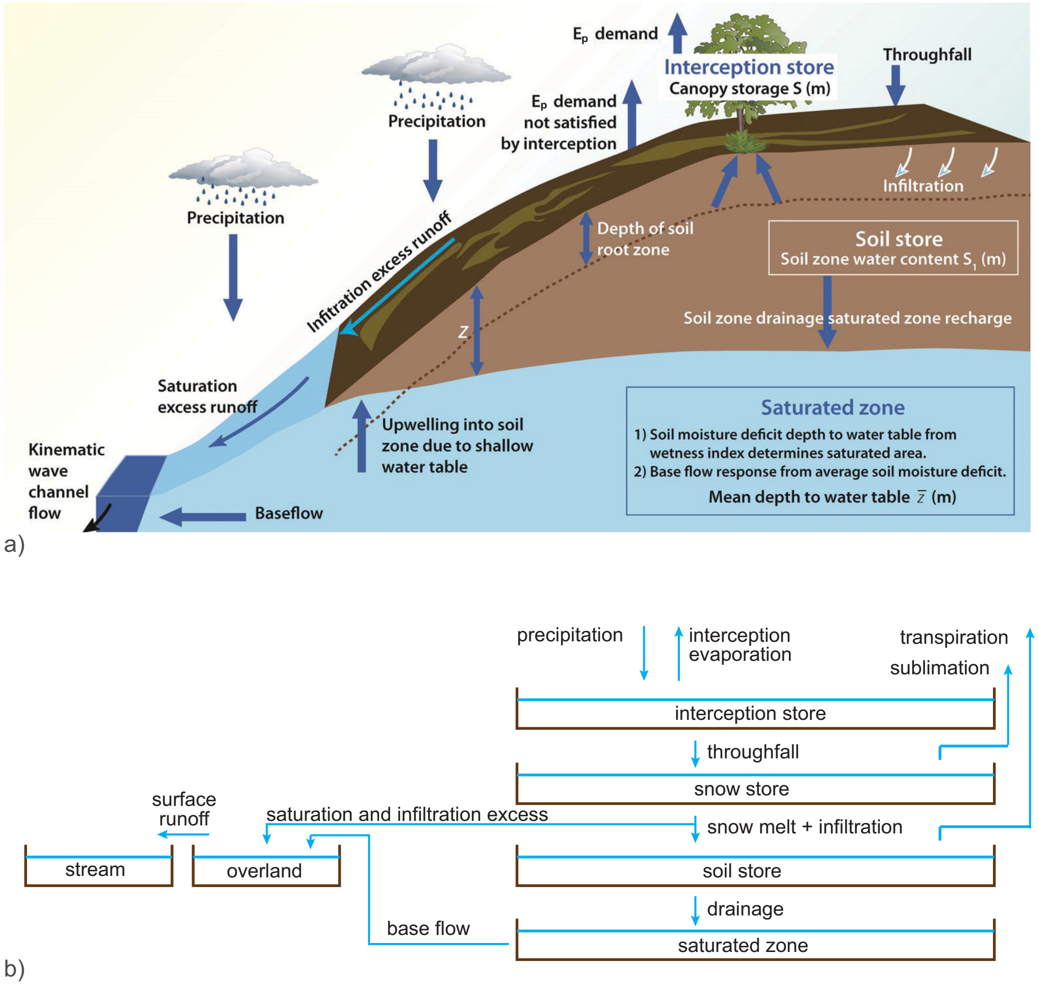

Figure 3. (a) Perceptual representation of TopNet (adapted from *Bandaragoda et al.* [2004]; © Elsevier Ltd.); (b) conceptual representation of TopNet.

available topography, land use, and soil data [*Clark et al.*, 2008]. The model conceptualization consists of five storage reservoirs and the closure relations between these storages (Figure 3; refer to *Clark et al.* [2008] for model equations and parameter explanations). Distributed calculations for all storages and fluxes are carried out for all third-order subcatchments (approx. 10 km^2): the underlying first-order streams are defined with an upstream area of 0.14 km^2. Discharges from each third-order subcatchment are then routed along the river network to calculate the discharge of the higher order catchments. Using TopNet with climate-derived S_r requires a transfer of $S_{r,clm}$ to a model parameter; $S_{r,clm}$ is transferred to the soil porosity corresponding to plant available water ($\Delta\theta_p$) (for details see section 3.2.2).

TopNet simulates third-order subcatchments, but the catchment representative $S_{r,clm}$ values were derived for fourth-order to seventh-order catchments; therefore, the catchment representative $S_{r,clm}$ needs to be disaggregated to these third-order subcatchments. In addition to the 40 years of catchment average data for the 32 catchments, 10 years of daily precipitation data and estimates of long-term mean annual discharge [*Woods et al.*, 2006] were also available for each third-order subcatchment. From the results presented in section 4, it follows that the catchment representative $S_{r,clm}$ shows a linear relation with the runoff coefficient (Figure 4a), where the runoff coefficient is tightly linked to the aridity index, as illustrated by the Budyko framework [*Budyko*, 1974] and therefore indicates the wet- or dryness of the catchment. A strong relationship between these two variables is expected because a smaller S_r estimate decreases the water available for transpiration, and therefore increases the runoff coefficient, as illustrated by previous studies [e.g., *Donohue et al.*, 2012; *Gao et al.*, 2014]. This dependency is used to proportionally disaggregate the catchment representative values to the third-order subcatchments. For the disaggregation, a linear relation

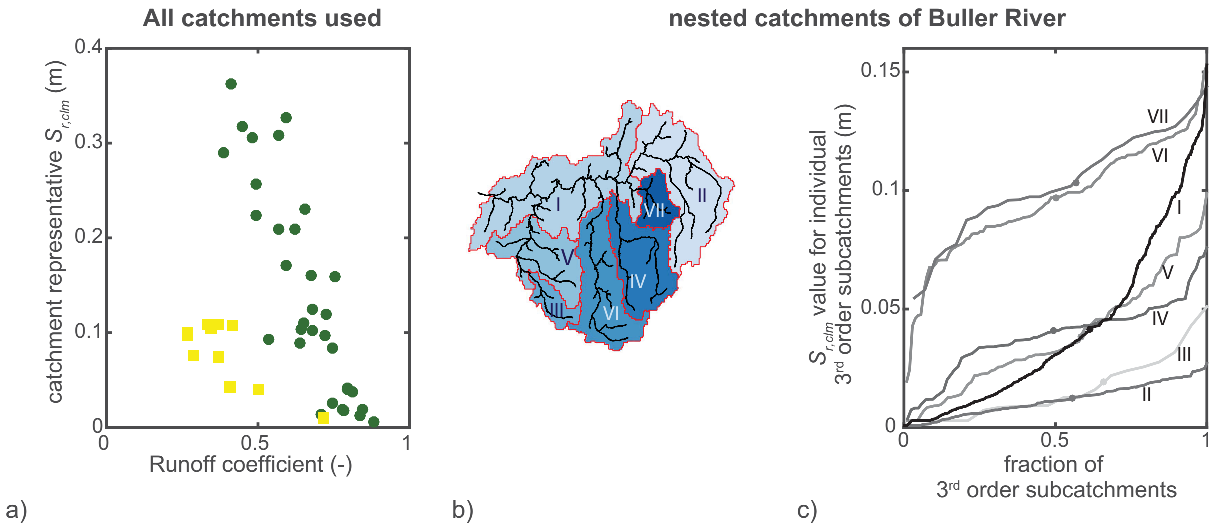

Figure 4. Summary of disaggregation method. (a) Relation between runoff coefficient and catchment representative $S_{r,clm}$ for catchments where dormancy is not dominant (green circles) or where dormancy is dominant (yellow squares). (b) Different nested catchments of Buller catchment. (c) Cumulative distribution of $S_{r,clm}$ values of third-order subcatchments for each nested basin in Figure 4b, characters refer to different nested catchments in Figure 4b; markers indicate the catchment representative value. Note that not all third-order subcatchments have an equal catchment area; thus, the catchment representative value is not always the average of the maximum and minimum value of the third-order subcatchments.

between $S_{r,clm}$ and the runoff coefficient (C_r) was assumed, while preserving the catchment representative $S_{r,clm}$; zero storage was set as boundary condition for C_r equals 1. In case of nested catchments, disaggregation was carried out from upstream to downstream, preserving the values assigned to the third-order subcatchments in the nested catchments. Figures 4b and 4c show an example of the disaggregation for the Buller catchment; it can be seen that the main catchment (I) spans all the $S_{r,clm}$ values occurring in the third-order subcatchments. Disaggregation was not necessary for $S_{r,soil}$, as these values were already estimated for first-order subcatchments and were averaged to third-order subcatchments according to catchment area.

Changing the root zone storage capacity in the model can influence the modeled catchment response at an event time scale and at longer, e.g., yearly, time scales. For instance at the event time scale, a smaller S_r causes a quick reduction of soil moisture deficits during events, leading to faster connectivity, as processes such as preferential flow are activated. As an effect of this the shapes of the peaks (effect 1a) and the event runoff coefficient (effect 1b) will change. At the yearly time scale, however, a smaller S_r decreases the storage and buffer capacity. This in turn affects the partitioning between discharge and evaporation (effect 2a), the flow variability between years (effect 2b) and the runoff volume during the dry season (effect 2c). These five effects (1a/1b/2a/2b/2c) were used to compare the discharges, modeled with $S_{r,soil}$ and $S_{r,clm}$. For each effect, one or more hydrological signatures were constructed (Table 3) and both modeled discharges were

Table 3. Overview of Used Signatures[a]

Signature	Metric	Effect	Source
Event time scale			
Median slope rising limb	E_{RE}	1a	
Median slope falling limb	E_{RE}	1a	
Slope of peak distribution	E_{RE}	1a	*Euser et al.* [2013]
Mean event runoff coefficient	E_{RE}	1b	*McMillan et al.* [2013]
Std event runoff coefficient	E_{RE}	1b	*McMillan et al.* [2013]
Correlation coefficient auto correlation (lag = 1 day)	E_{RE}	1a	*Winsemius et al.* [2009]
Yearly time scale			
Average base flow (lowest 5% of flow)	E_{RE}	2c	
Slope of normalized flow duration curve	E_{RE}	2c	
Runoff coefficient	E_{RE}	2a	
Std yearly discharge	E_{RE}	2b	
Discharge	E_{NSE}	NA	*Nash and Sutcliffe* [1970]
Discharge	E_{VE}	NA	*Criss and Winston* [2008]

[a]The process numbers indicate for which runoff process a signature is selected: the signatures do not only evaluate this process but have a strong focus toward this process (E_{RE} = relative error [*Euser et al.*, 2013], E_{NSE} = Nash-Sutcliffe efficiency, and E_{VE} = volume error).

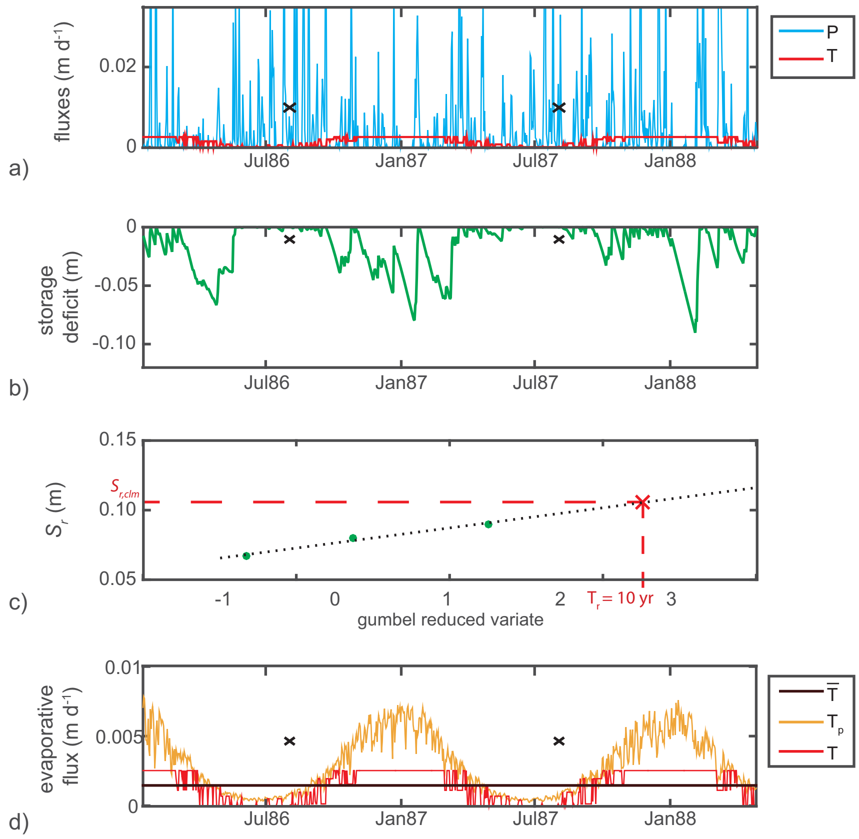

Figure 5. Method for climate-derived root zone storage capacity; (a) precipitation and estimated transpiration; (b) calculated soil moisture deficit; (c) use of yearly minimum storage in Gumbel distribution; and (d) use of potential transpiration to estimate actual transpiration. Black crosses indicate the start of a simulation year.

evaluated on their ability to reproduce these observed signatures. In addition to the listed signatures also the Nash-Sutcliffe efficiency (E_{NSE}) [*Nash and Sutcliffe*, 1970] and volume error (E_{VE}) [*Criss and Winston*, 2008] of the discharge are used in the comparison. All signatures were combined into an integrated performance measure by using the Euclidian distance to the "perfect model," i.e., metrics being zero (D_E; equation (1)) [*Hrachowitz et al.*, 2014]; this integrated measure was used to evaluate the overall effect of changing S_r.

$$D_E=\sqrt{\frac{sum_{n=1}^{N}(1-E_n)^2}{N}}, \tag{1}$$

where E_n is the performance metric of signature n and N is the total number of signatures (including E_{VE} and E_{NSE}).

3.2. Derivation of S_r Values

3.2.1. Climate-Derived $S_{r,clm}$

For the climate-derived root zone storage capacity ($S_{r,clm}$), we assumed that transpiration will deplete the root zone storage during dry spells. To estimate the root zone storage capacity, we assume that vegetation reserves a storage large enough to overcome a dry spell with a certain return period. To estimate the required annual storages, a simplified water balance model was introduced; one with only an interception and root zone storage reservoir [e.g., *Fenicia et al.*, 2008] and only one parameter (max. interception storage capacity) and no further closing relations. The root zone storage reservoir has zero moisture deficit at the beginning of the simulation (i.e., end of the wet period) and the deficit increases when transpiration exceeds net precipitation ($P-E_i$) (Figures 5a and 5b); any excess precipitation is assumed to runoff directly. The simulation was carried out for each catchment for the entire length of the precipitation series (1972–2012) on a daily basis. By doing this simulation, the yearly maximum deficits can be determined, which are

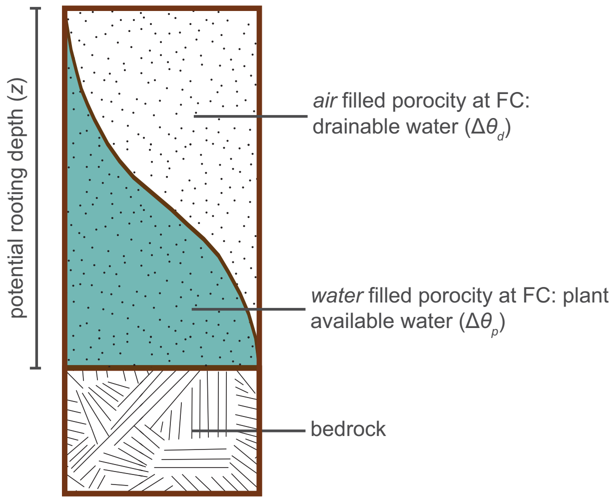

Figure 6. Method for soil-derived root zone storage capacity (FC = field capacity).

equivalent to the root zone storage capacities required to maintain a sufficient supply of water to vegetation during dry periods and to thereby fulfill the evaporative demand in the individual years.

Following the daily simulation, the Gumbel extreme value distribution was used to standardize the results from different catchments [*Gumbel*, 1935]. The maximum moisture deficits of the individual years are used as input into the extreme value distribution (Figure 5c). From this distribution, the root zone storage capacities can be estimated which are necessary for vegetation to bridge dry spells with specific return periods. The results from *Gao et al*. [2014] suggest that many ecosystems tend to develop root zone storage capacities large enough to survive dry spells with return periods between 10 and 20 years; it is likely that grasses are adapted to lower return periods. Therefore, the analysis here is based on S_r values belonging to dry spells with return periods of 10 years, section 5.1 shows a sensitivity analysis regarding the chosen return period.

An estimate for *actual* transpiration (T) is required before the analysis described above can be carried out. Transpiration is estimated based on the long-term water balance and estimates of potential evaporation (Figure 5d). The long-term average transpiration ($\overline{T}$) is derived from the water balance:

$$\overline{T} = \overline{P - E_i} - \overline{Q}, \tag{2}$$

where P is precipitation, E_i is interception evaporation, and Q is observed discharge. Interception evaporation is determined by simulating an interception reservoir, accounting for interception storage, effective rainfall (throughfall) and interception evaporation. Maximum interception storages were taken from the TopNet configuration, they depend on land cover and range from 0.5 mm for pasture to 1.9 mm for forest. The influence of these values was evaluated in a sensitivity analysis (section 5.1). The required root zone storage capacity is set to zero when discharge equals net precipitation ($P - E_i$), which would theoretically occur in the absence of evaporative demand or when no more storage is available. For estimating the transpiration, only those hydrological years were used, which had complete discharge data.

Transpiration is not constant over the year; therefore, potential transpiration ($T_p = \overline{E_p} - E_i$) is used to add seasonality to the long-term average transpiration ($\overline{T}$). When $\overline{T}$ exceeds daily T_p (in winter), T equals T_p (Figure 5d). By doing this, some evaporative energy of $\overline{T}$ is not assigned to T in the winter period, so to close the water balance, this energy is equally redistributed over the months in which T_p exceeds $\overline{T}$ (in summer). Seasonality in transpiration is caused not only by seasonality in potential transpiration but also by vegetation going into a state of dormancy. The latter is assumed to occur in catchments classified as dry and with a pasture land cover. During the summer months (December till March), the grass in these catchments turns yellow and does not transpire. Therefore, transpiration is set to zero during the summer months for these catchments. The influence of this dormancy on $S_{r,clm}$ is evaluated with a sensitivity analysis (section 5.1).

3.2.2. Soil-Derived $S_{r,soil}$

Existing, national estimates of soil-derived root zone storage capacity ($S_{r,soil}$) are available for the study catchments, based on the available storage between wilting point and field capacity. The soil moisture depth corresponding to wilting point and field capacity was derived from field measurements: water and air filled porosity at field capacity and potential rooting depth (Figure 6) were observed for different soils and locations in New Zealand. The characteristics of different soils were used to estimate the soil moisture depth at field capacity and wilting point for all first-order catchments in New Zealand [*Newsome et al*., 2008; *Webb and Wilson*, 1995]. These values are currently used for the uncalibrated and distributed version of the national hydrological model TopNet. Specifically, $S_{r,soil}$ is here inferred from the model parameters in TopNet

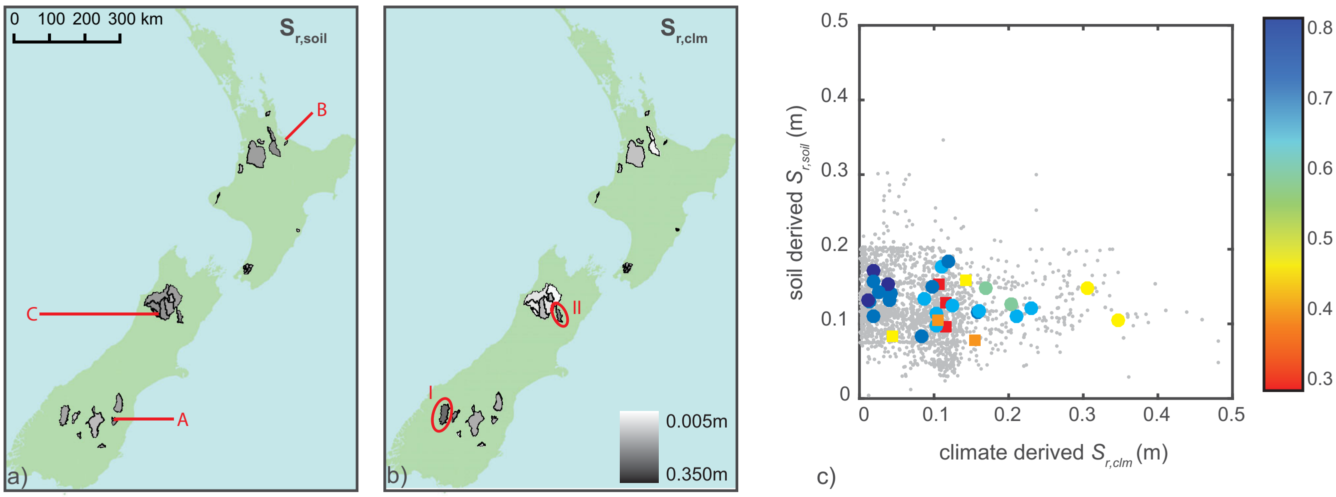

Figure 7. Catchment representative S_r values for selected catchments A, B, and C (see Table 2 for more details); (a) soil-derived $S_{r,soil}$; (b) climate-derived $S_{r,clm}$; (c) scatterplot, the catchment representative S_r values from Figures 7a and 7b are color coded by runoff coefficient (circles = no dormancy and squares = dormancy), grey dots show S_r values per third-order subcatchment.

representing the potential rooting depth (z) and the fraction of plant available water ($\Delta\theta_p$, water filled porosity at field capacity), by using equation (3).

$$S_r = z * \Delta\theta_p. \tag{3}$$

4. Results

4.1. Comparison of S_r Values

4.1.1. Spatial Patterns

Figure 7 shows the comparison between $S_{r,clm}$ and $S_{r,soil}$. It can be seen that $S_{r,clm}$ is lower than $S_{r,soil}$ for the areas classified as "wet" or "extremely wet" (Figure 1). For the dryer areas, the values are more comparable, but with slightly higher values for $S_{r,clm}$.

The same interpretation follows from Figure 7c, which shows a scatterplot between $S_{r,clm}$ and $S_{r,soil}$ for catchment representative values (the ones shown in Figures 7a and 7b), and for values for each subcatchment of at least third-order (the individual subcatchments in TopNet). It can be seen that $S_{r,clm}$ is correlated with the runoff coefficients and that the range in $S_{r,clm}$ is larger than the range in $S_{r,soil}$. The relation between $S_{r,clm}$ and runoff coefficient is less pronounced for catchments where grass dormancy is important. The latter is probably an artifact of the dormancy assumption: transpiration is set to zero in summer, meaning that transpiration must be higher in winter to close the water balance. However, this is not incorporated in the analysis (see also section 5.1).

Although Figures 4 and 7c show that the runoff coefficient has a strong control on $S_{r,clm}$, the figures also show it is not the only controlling factor. Other factors can be interstorm duration, seasonality, and yearly rainfall depth [*Gao et al.*, 2014]. An example can be found on the South Island: $S_{r,clm}$ for catchments I and II (indicated with red circles) is higher than the values for the dry catchments and extremely wet catchments, while they have a runoff coefficient larger than the dry and smaller than the extremely wet catchments. A possible reason for their high $S_{r,clm}$ is that although they are classified as wet, their precipitation surplus is much smaller than for the average wet catchments (Figure 2). But because they are classified as wet, the vegetation is assumed not to undergo dormancy and therefore to require sufficient soil water to maintain transpiration through the summer (*Wang-Erlandsson et al.*, 2016) (see also section 5.1).

4.2. Comparison of Model Results

4.2.1. Hydrographs

Figure 8 shows the observed and modeled hydrographs for three contrasting catchments: one where soil has more explanatory power (i.e., using $S_{r,soil}$ gives more accurate results) (a), one where soil and climate give similar results (b), and one where climate has more explanatory power (c). Details about these

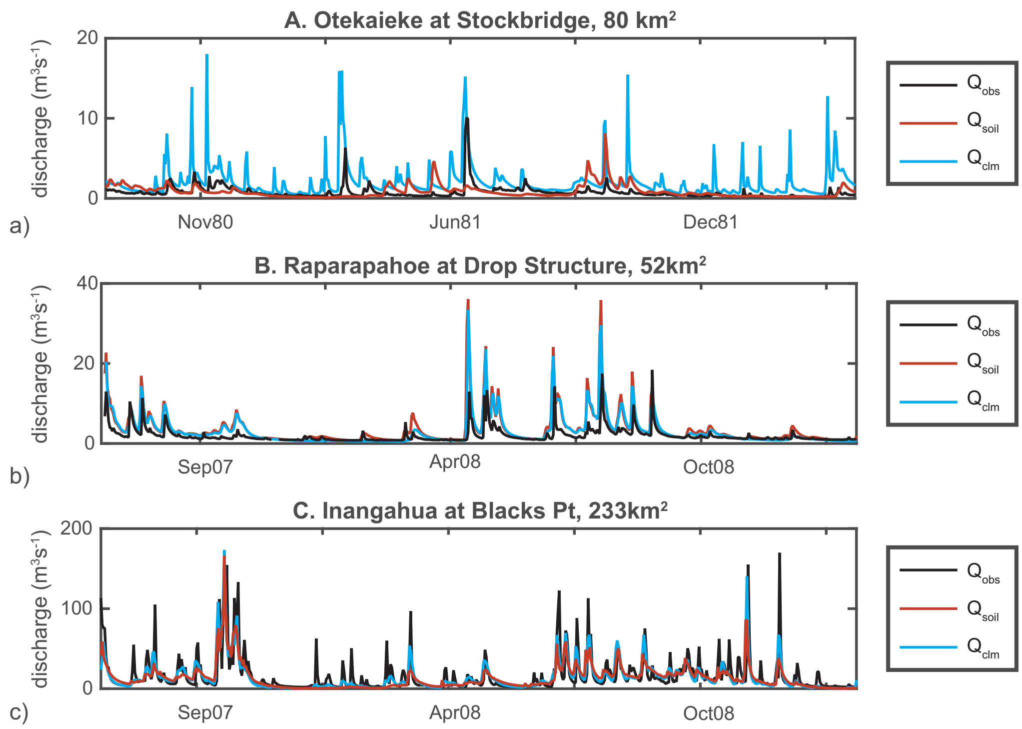

Figure 8. Observed and modeled discharge for both methods for three catchments; (a) $S_{r,soil}$ better (Otekaieke at Stockbridge, Otago); (b) $S_{r,soil}$ and $S_{r,clm}$ in balance (Raparapahoe at above drop structure, Bay of Plenty); (c) $S_{r,clm}$ better (Inangahua at Blacks pt, West Coast). For details about the catchments refer to Table 2.

catchments, including derived S_r values can be found in Table 2. The figure indicates that replacing $S_{r,soil}$ by $S_{r,clm}$ can have different effects: $S_{r,soil}$ is similar for all three catchments while $S_{r,clm}$ strongly varies. For the top plot, a small change in S_r causes considerable changes in the responsiveness of the catchment, while for the middle plot, even a doubled S_r has only a limited influence on the modeled discharge. In the bottom plot, in contrast, a decrease in S_r leads to a flashier flow; however, to match the responsiveness of the observed flow, $S_{r,clm}$ should decrease even more.

Although the results in Figure 8 show reasonable matches between the modeled and observed flow, they also contain some clear shortcomings. Figure 8 for example shows that because the model is not calibrated or tailored for the specific catchments, some observed features are still poorly reproduced by the model. Replacing $S_{r,soil}$ by $S_{r,clm}$ does not change the reproduction of these features, which indicates that these features are dominated by other (poorly identified) parameters [*Clark et al*., 2008; *Booker and Woods*, 2014].

4.2.2. Specific Signatures

Figure 9 shows the values of two signatures for all catchments for the observed and the two modeled cases. The catchments are ordered by increasing observed runoff coefficient in both plots; it can be seen that high runoff coefficients do not always coincide with high slopes of the rising limb, although generally, the catchments with lower runoff coefficients have lower slopes for their rising limbs. The signature values for the two modeled cases are either both too high or both too low for the majority of the catchments and for both signatures, demonstrating that the value of S_r is only part of the control on these signatures. Despite this, the model with $S_{r,clm}$ can better reproduce these two signatures for a slight majority of the catchments. Further it follows from the graph that the model is better able to reproduce the variability in slope of rising limbs than the variability in runoff coefficients, irrespective of using soil or climate data to estimate S_r.

4.2.3. Combination of Signatures

By combining the results of all signatures and catchments, an overall comparison between soil-derived and climate-derived S_r values can be made. Figure 10 shows whether a signature (rows) can be better reproduced with $S_{r,soil}$ (red squares) or $S_{r,clm}$ (blue dots) for each catchment (columns). The shading of the symbols indicates the difference between $S_{r,clm}$ and $S_{r,soil}$; the absence of a symbol indicates no significant difference

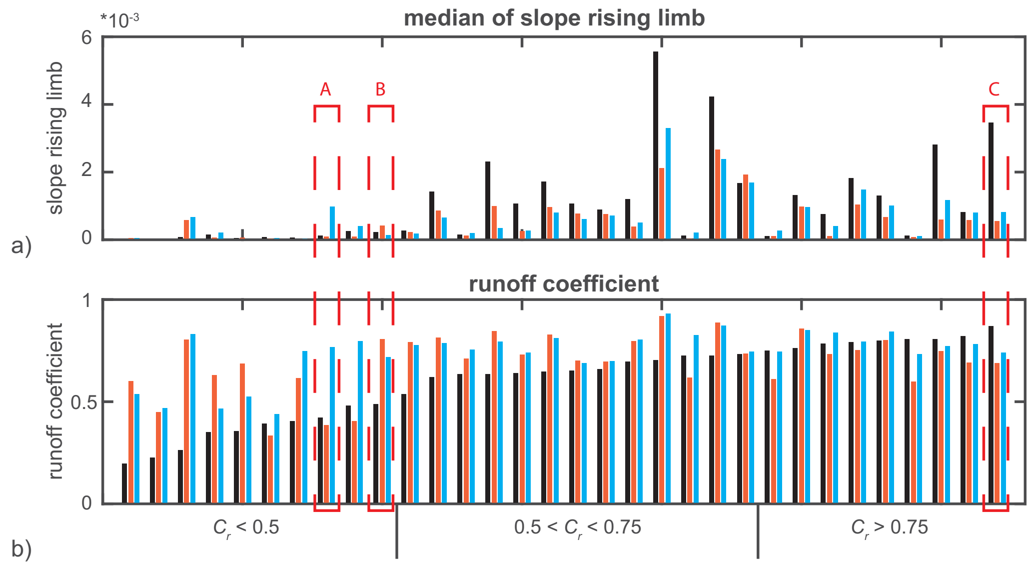

Figure 9. Reproduction of a selection of the used signatures, both plots are ordered by increasing runoff coefficient; red rectangles indicate catchments presented in Figure 8 (black (first) bar = observed, red (second) bar = soil, and blue (third) bar = climate); (a) Median of slope of rising limb; (b) long-term runoff coefficient.

between $S_{r,clm}$ and $S_{r,soil}$. It can be seen that the differences between $S_{r,soil}$ and $S_{r,clm}$ are largest for dryer catchments (left side); differences are smallest for the intermediate catchments (C_r between 0.5 and 0.75). Further, the figure shows that for the dry and intermediate catchments $S_{r,soil}$ and $S_{r,clm}$ perform equally well (48 red versus 57 blue and 35 red versus 35 blue, respectively), while for the wet catchments, $S_{r,clm}$ strongly outperforms $S_{r,soil}$ (15 red versus 49 blue). Regarding the signatures, Figure 10 shows that the differences between $S_{r,clm}$ and $S_{r,soil}$ are larger for those focusing on the event time scale (lower part of graph) and thus the shape of the peaks, i.e., the short-term memory of the system. The differences are smaller for the signatures focusing on the longer time scale (top part of graph). A reason for this could be that the root zone storage is more important for the high frequency processes, which have a stronger existence in the event time scale (i.e., overland flow) than in the yearly time scale (i.e., base flow) [*Oudin et al.*, 2004; *Euser et al.*, 2015].

The top row in Figure 10b shows the Euclidean distance (equation (1)) as an overall performance measure, integrating all signatures for each catchment. The overall performance exhibits the same pattern as the individual signatures: while either climate-derived or soil-derived S_r may perform better for the drier catchments, depending on the specific catchment, little differences were found for the intermediate catchments. In contrast, the results strongly suggest that climate has considerably more explanatory power for the wet catchments. The median difference in Euclidean distance to the perfect model is 0.11 in favour of $S_{r,soil}$, 0.1 in favour of $S_{r,clm}$ and 0.05 in favour of $S_{r,clm}$ for low, middle and high C_r respectively. Figure 10a further underlines that the higher variability of $S_{r,clm}$ and thus in particular the very low values derived for wet catchments contribute to consistently higher model skill in these catchments. More generally, it can be seen that $S_{r,clm}$ outperforms $S_{r,soil}$ when the first is larger for the drier catchments and when $S_{r,clm}$ is lower for the wetter catchments. We suggest that this is because the soil-derived values have similar ranges of magnitude for all catchments, and do not, at least at the time scales of hydrological interest, have a relationship with climate. However, for wet catchments the precipitation deficits, if any, are smaller during the drier summer period than for dry catchments (Figure 2). Thus, vegetation does not need to make use of the full soil depth, and therefore the soil-derived values are too large to be used in a hydrological model. In such wet catchments, climate-derived values result in improved model performance.

5. Discussion

5.1. Application of Climate Method

By using the described climate method, we hypothesize that vegetation adapts its rooting system according to the storage required by the evaporative demand, leading to smaller storage capacities in wet areas

Figure 10. (a) Soil-derived (red squares) and climate-derived (blue circles) S_r, catchments are ordered by increasing runoff coefficient. (b) Overview of signature scores: blue circles and red squares indicate that a specific signature can be better reproduced with $S_{r,clm}$, respectively, $S_{r,soil}$ for a specific catchment. Where no dots are shown, the performance difference for the specific signature between the two methods is smaller than 0.03. The shading of the symbols from dark to light indicates the degree of performance difference by using $S_{r,clm}$ and $S_{r,soil}$. The performance differences are categorized by >0.5 (darkest), 0.2–0.5 (middle), 0.03–0.2 (lightest), <0.03 (no symbol). Signatures on top focus more on long-term water balance, while signatures at the bottom focus more on peak shape and height. The arrows indicate the catchments used in Figure 8.

and larger capacities in dry areas. This is hypothesized because in wetter areas, the periods are generally shorter in which the evaporative demand exceeds the precipitation and characterized by a smaller precipitation deficit than for drier areas. This hypothesis would also imply that the medium-term dynamics of climatic variability can be found in the medium-term dynamics of root development, and thus in root zone storage capacities. The results show that the differences in $S_{r,clm}$ between catchments are larger than the differences in $S_{r,soil}$ between catchments and that a model with $S_{r,clm}$ has a higher performance for a majority of the catchments. To apply the climate-based method, several assumptions need to be made which may influence the derived root zone storage capacity, concerning grass dormancy, the return period, and interception storage. Figure 11 shows a sensitivity analysis regarding these assumptions for a subset of catchments containing dry and wet catchments (Table 2). The influence of dormancy was not tested for the extremely wet catchment, as it is not relevant under such conditions.

Figure 11 shows that the assumption regarding grass dormancy has the largest influence on the derived $S_{r,clm}$. In the current study, the effect of dormancy is applied by setting transpiration to zero instantaneously from December to March for dry catchments with grass land cover. In contrast to the redistributed "winter evaporative energy" (section 3.2.1), this energy is not redistributed in the remainder of the year. The large uncertainty in $S_{r,clm}$ in these catchments therefore may explain the lower performance for these catchments: often the modeled discharge is too high and too responsive. This indicates that the derived $S_{r,clm}$ is too small and that setting transpiration to zero during dry summers probably results in underestimation of transpiration. Another reason for the inferior results in dry catchments is likely to be that grass does not go into dormancy instantaneously, but rather gradually [e.g., *Ofir and Kigel*, 1999]. In addition, a longer rain event in summer can lead to partial activation of transpiration of grass again. If these effects are reflected in the transpiration, larger values of $S_{r,clm}$ will be derived for these catchments.

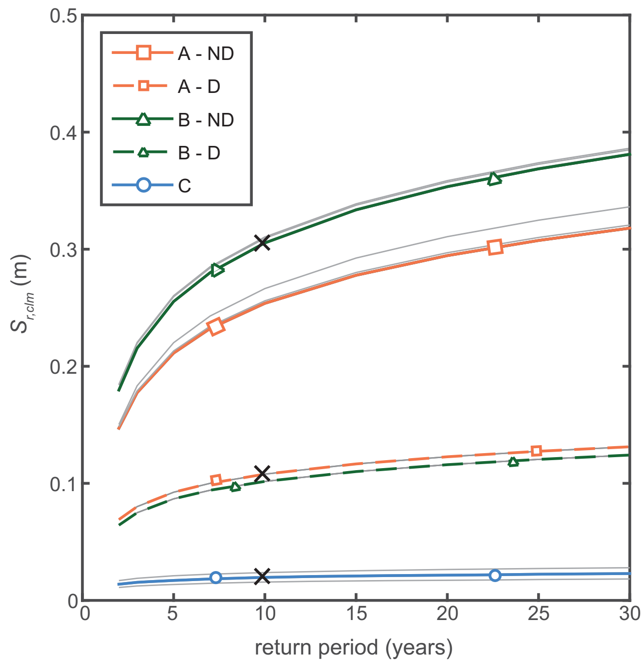

Figure 11. Sensitivity analysis for the subset of catchments: A is a dry, B a wet, and C an extremely wet catchment (for more details see Table 2). Colored lines show the $S_{r,clm}$ values for the interception capacity used during the entire analysis, the grey lines show the $S_{r,clm}$ values for an interception capacity which is 0.5 mm smaller or larger. The black crosses indicate the $S_{r,clm}$ values used in the analyses (ND = without dormancy and D = with dormancy).

During this study, a return period of 10 years was chosen, following *Gao et al.* [2014] and resulting in values in the same range as the soil-derived values. Figure 11 shows that especially for dryer areas, S_r strongly depends on the selected return period, while this relation is much weaker for wet catchments. This makes it possible to derive more stable values of $S_{r,clm}$ for wet catchments than for dry catchments, which is likely to result in better model results. On the other hand, Figure 10 shows that $S_{r,clm}$ should probably be slightly smaller than the 10 year value for wet catchments (shorter return period) and larger for dry catchment (longer return period). The reason for the former may be that in wetter areas, it is more likely that water is available at depths that can be reached by plant roots within a feasible period of time.

The influence on $S_{r,clm}$ of the chosen maximum interception storage is relatively small (Figure 11), especially for the dryer catchments (grey lines coincide with colored lines). For the wetter catchments, the maximum interception storage has a larger influence, but still a smaller influence than dormancy or return period in dryer catchments. Surprisingly, the derived $S_{r,clm}$ values for a higher and lower maximum interception storage are both higher than the $S_{r,clm}$ value used during the study in case of no dormancy. For the lower interception capacity, this is as expected; for the higher interception capacity, it is caused by the decrease of potential transpiration.

Although some assumptions have a strong influence on the derived $S_{r,clm}$ in the dry catchments, relatively stable $S_{r,clm}$ values can be derived for wet catchments. This indicates that the hypothesis that vegetation dynamically creates its root zone storage capacity as a function of climatic variability is plausible, which is underpinned by the fact that the model with $S_{r,clm}$ gives better results than the model with $S_{r,soil}$ for a majority of the catchments, and in particular the wetter catchments. The larger influence of the assumptions in the dryer catchments does not imply that the general hypothesis needs to be rejected for dryer areas; it only means that the detailed assumptions of the climate method should be carefully revisited in these areas.

An important advantage of the present approach is that it allows for the incorporation of medium time scale evolution of the root system with changes in climatic forcing in models. Currently, this is hardly reflected in hydrological modeling experiments [e.g., *Breuer et al.*, 2003; *Ivanov et al.*, 2008], while the medium time scale in climatic variability is considered to be very important. Considering the root zone storage as a dynamic instead of a static system can increase our understanding of how the system works, which is necessary to predict how a system may respond to disturbances such as climate change [*Troch et al.*, 2015].

5.2. Influence of Data Quality

$S_{r,soil}$ and $S_{r,clm}$ are both based on a set of data; errors in these data sources can have different effects on the derived values and the comparison between the two. One of the main data sources for $S_{r,clm}$ is precipitation. An underestimation of the precipitation, which is more likely to occur in the wet mountainous areas, would lead to an underestimation of $\overline{T}$. The influence on the required storage, on the other hand, will be smaller, as both precipitation and transpiration are smaller.

The quality of the soil data to a large extent depends on the spatial resolution of the measurements. The soil data were not originally collected for countrywide rainfall runoff predictions, but rather as supporting information for agricultural practices, as in most places around the world. Therefore, it can be expected that the derived $S_{r,soil}$ is more reliable for the flatter agricultural areas, where it is easier to collect data, than for the mountainous forested areas. In the latter areas, the climate method currently strongly outperforms the soil method; thus, this could be due to either a better representation by the climate method (with stable values in wet areas) or poorer data quality for the soil method. Irrespective of the reason, this performance difference clearly highlights the value of the climate method: with less (field) effort conceptually more adequate estimates can be achieved.

5.3. Model Effects and Implications

Not only values of storage capacities but also model results were compared for this study. In general, the outcome of the comparison of model results depends on the selected models and on how the newly derived values are incorporated in the model. Here the uncalibrated version of TopNet was used, implying that parameters were estimated based on countrywide observed data. An uncalibrated model has the disadvantage that it does not perform very well in all catchments [*Booker and Woods*, 2014]. On the other hand, the advantage is that the other model parameters are not tuned toward a specific $S_{r,soil}$, therefore replacing only S_r creates a more equal comparison than would be the case for a calibrated model. It should be noted that the long-term average observed discharge was used to derive $S_{r,clm}$; the modelled discharges were then compared to the same discharge observations, leading to a small dependency between $S_{r,clm}$ and the observed discharge.

5.4. Applicability in Ungauged Catchments

Understanding the hydrological behavior of a catchment is important, both if the catchment is well gauged (like those used for this study), or if it is poorly gauged (like the majority of catchments worldwide) [*Hrachowitz et al.*, 2013]. The climate method described here does considerably improve understanding even of ungauged catchments. Although no discharge data are available for these catchments, estimates of S_r can be obtained from precipitation and evaporation data readily available worldwide from remote sensing products. This information is becoming more widely available and *Wang-Erlandsson et al.* [2016] have shown that when using these products very plausible worldwide estimates for S_r can be derived.

5.5. Variables Influencing S_r

This study compares the relative influence of soil and climate on the root zone storage capacity. However, more factors influence S_r in addition to soil and climate. These factors are plant physiology, nutrient availability, plant competition, and alternative plant survival strategies (e.g., a cactus plant stores water in its body systems); these factors can have large influences and in some cases overrule the influence of soil and climate. It is worth noting that any of these other factors have to be measured at point scale and therefore create the need for upscaling, which is not necessary for the climate method.

Although the described climate method is an engineering approach, it is based on the principle of coevolution: vegetation strives to create an optimal environment and if this is not possible, the vegetation may not grow at the specific location. This notably implies that the suggested climate method is probably less suitable in areas where humans continually influence the vegetation, such as managed areas with (annual) crops.

6. Conclusions

This study shows a comparison between soil-derived and climate-derived root zone storage capacity (S_r). S_r values from climate and soil were compared directly as well as via hydrological model results for 32 contrasting catchments in New Zealand. The key findings are that climate-derived S_r values on balance outperform soil-derived values for most natural catchments, based on multiple metrics. For drier catchments, the differences in model results with S_r estimates from soil and climate are larger than for wetter catchments. In wetter catchments, climate-derived S_r values clearly outperform soil-derived values, despite smaller absolute differences in performance. Thus, we can conclude that climate data have a higher explanatory power for S_r than soil data, this higher explanatory power allows for taking into account the medium-term development of catchment vegetation. Combining the medium-term dynamics and the easier accessibility of data makes the climate-derived S_r a valuable addition to hydrological and climate models and opens doors to evaluate changes in catchment response within a changing climate.

Acknowledgments
This work has been conducted with funding from Rijkswaterstaat, Netherlands. We thank Rijkswaterstaat for their support. We thank NIWA and the NZ Regional Councils for access to meteorological and discharge data. We thank Axel Kleidon and two anonymous reviewers for their detailed comments, which helped us to strengthen the manuscript. All underlying data are available on request from the first author except for measured flow data which can be requested from the NZ Regional Council measurement authorities, contact details also available from the first author.

References

Bandaragoda, C., D. G. Tarboton, and R. Woods (2004), Application of TOPNET in the distributed model intercomparison project, *J. Hydrol.*, *298*(1–4), 178–201.

Beekman, W., R. Caljé, F. Schaars, and J. Heijkers (2014), Vergelijking van enkele schattingsmethoden voor de actuele verdamping, *Stromingen*, *20*, 227–239.

Beven, K. (2006), A manifesto for the equifinality thesis, *J. Hydrol.*, *320*(1–2), 18–36.

Booker, D., and R. Woods (2014), Comparing and combining physically-based and empirically-based approaches for estimating the hydrology of ungauged catchments, *J. Hydrol.*, *508*, 227–239.

Breuer, L., K. Eckhardt, and H.-G. Frede (2003), Plant parameter values for models in temperate climates, *Ecol. Modell.*, *169*(2–3), 237–293.

Brunner, I., C. Herzog, M. A. Dawes, M. Arend, and C. Sperisen (2015), How tree roots respond to drought, *Front. Plant Sci.*, *6*, 547.

Budyko, M. I. (1974), *Climate and Life*, 508 pp., Academic Press, N. Y.

Camporese, M., E. Daly, and C. Paniconi (2015), Catchment-scale Richards equation-based modeling of evapotranspiration via boundary condition switching and root water uptake schemes, *Water Resour. Res.*, *51*, 5756–5771, doi:10.1002/2015WR017139.

Canadell, J., R. B. Jackson, J. B. Ehleringer, H. A. Mooney, O. E. Sala, and E.-D. Schulze (1996), Maximum rooting depth of vegetation types at the global scale, *Oecologia*, *108*(4), 583–595.

Cassiani, G., J. Boaga, D. Vanella, M. T. Perri, and S. Consoli (2015), Monitoring and modelling of soilplant interactions: The joint use of ERT, sap flow and eddy covariance data to characterize the volume of an orange tree root zone, *Hydrol. Earth Syst. Sci.*, *19*, 2213–2225.

Clark, M. P., D. E. Rupp, R. A. Woods, X. Zheng, R. P. Ibbitt, A. G. Slater, J. Schmidt, and M. J. Uddstrom (2008), Hydrological data assimilation with the ensemble Kalman filter: Use of streamflow observations to update states in a distributed hydrological model, *Adv. Water Resour.*, *31*(10), 1309–1324.

Criss, R. E., and W. E. Winston (2008), Do Nash values have value? Discussion and alternate proposals, *Hydrol. Processes*, *22*(14), 2723–2725.

Crow, W. T., A. A. Berg, M. H. Cosh, A. Loew, B. P. Mohanty, R. Panciera, P. de Rosnay, D. Ryu, and J. P. Walker (2012), Upscaling sparse ground-based soil moisture observations for the validation of coarse-resolution satellite soil moisture products, *Rev. Geophys.*, *50*, RG2002, doi:10.1029/2011RG000372.

Dirmeyer, P. A. (2011), The terrestrial segment of soil moisture-climate coupling, *Geophys. Res. Lett.*, *38*, L16702, doi:10.1029/2011GL048268.

Donohue, R. J., M. L. Roderick, and T. R. McVicar (2012), Roots, storms and soil pores: Incorporating key ecohydrological processes into Budykos hydrological model, *J. Hydrol.*, *436–437*, 35–50.

Eagleson, P. S. (1982), Ecological optimality in water-limited natural soil-vegetation systems: 1. Theory and hypothesis, *Water Resour. Res.*, *18*(2), 325–340.

Euser, T., H. C. Winsemius, M. Hrachowitz, F. Fenicia, S. Uhlenbrook, and H. H. G. Savenije (2013), A framework to assess the realism of model structures using hydrological signatures, *Hydrol. Earth Sys. Sci.*, *17*(5), 1893–1912.

Euser, T., M. Hrachowitz, H. Winsemius, and H. Savenije (2015), The effect of forcing and landscape distribution on performance and consistency of model structures, *Hydrol. Processes*, *29*, 3727–3743.

Fenicia, F., H. H. G. Savenije, P. Matgen, and L. Pfister (2008), Understanding catchment behavior through stepwise model concept improvement, *Water Resour. Res.*, *44*, W01402, doi:10.1029/2006WR005563.

Fenicia, F., H. H. G. Savenije, and Y. Avdeeva (2009), Anomaly in the rainfall-runoff behaviour of the Meuse catchment. Climate, land-use, or land-use management?, *Hydrol. Earth Syst. Sci.*, *13*(9), 1727–1737.

Field, C. B., F. S. Chapin, P. A. Matson, and H. A. Mooney (1992), Responses of terrestrial ecosystems to the changing atmosphere: A resource-based approach, *Annu. Rev. Ecol. Syst.*, *23*, 201–235.

Gao, H., M. Hrachowitz, S. J. Schymanski, F. Fenicia, N. Sriwongsitanon, and H. H. G. Savenije (2014), Climate controls how ecosystems size the root zone storage capacity at catchment scale: Root zone storage capacity in catchments, *Geophys. Res. Lett.*, *41*, 7916–7923, doi:10.1002/2014GL061668.

Gentine, P., P. D'Odorico, B. R. Lintner, G. Sivandran, and G. Salvucci (2012), Interdependence of climate, soil, and vegetation as constrained by the Budyko curve, *Geophys. Res. Lett.*, *39*, L19404, doi:10.1029/2012GL053492.

Gharari, S., M. Hrachowitz, F. Fenicia, H. Gao, and H. H. G. Savenije (2014), Using expert knowledge to increase realism in environmental system models can dramatically reduce the need for calibration, *Hydrol. Earth Sys. Sci.*, *18*(12), 4839–4859.

Gimbel, K., H. Puhlmann, and M. Weiler (2015), Does drought alter hydrological functions in forest soils? An infiltration experiment, *Hydrol. Earth Sys. Sci. Discuss.*, *12*, 7689–7725.

Gumbel, E. (1935), Les valeurs extrmes des distributions statistiques, *Ann. l'I. H. P.*, *5*(2), 115–158.

Hrachowitz, M., et al. (2013), A decade of Predictions in Ungauged Basins (PUB)—A review, *Hydrol. Sci. J.*, *58*(6), 1198–1255.

Hrachowitz, M., O. Fovet, L. Ruiz, T. Euser, S. Gharari, R. Nijzink, J. Freer, H. H. G. Savenije, and C. Gascuel-Odoux (2014), Process consistency in models: The importance of system signatures, expert knowledge, and process complexity, *Water Resour. Res.*, *50*, 7445–7469, doi:10.1002/2014WR015484.

Ivanov, V. Y., R. L. Bras, and E. R. Vivoni (2008), Vegetation-hydrology dynamics in complex terrain of semiarid areas: 2. Energy-water controls of vegetation spatiotemporal dynamics and topographic niches of favorability, *Water Resour. Res.*, *44*, W03430, doi:10.1029/2006WR005595.

Kleidon, A., and M. Heimann (1998), A method of determining rooting depth from a terrestrial biosphere model and its impacts on the global water and carbon cycle, *Global Change Biol.*, *4*(3), 275–286.

Kleidon, A., and M. Heimann (2000), Assessing the role of deep rooted vegetation in the climate system with model simulations: Mechanism, comparison to observations and implications for Amazonian deforestation, *Clim. Dyn.*, *16*(2–3), 183–199.

Liancourt, P., A. Sharkhuu, L. Ariuntsetseg, B. Boldgiv, B. R. Helliker, A. F. Plante, P. S. Petraitis, and B. B. Casper (2012), Temporal and spatial variation in how vegetation alters the soil moisture response to climate manipulation, *Plant Soil*, *351*(1–2), 249–261.

McMillan, H., M. Gueguen, E. Grimon, R. Woods, M. Clark, and D. E. Rupp (2013), Spatial variability of hydrological processes and model structure diagnostics in a 50 km^2 catchment, *Hydrol. Processes*, *28*(18), 4896–4913.

Milly, P. (1994), Climate, interseasonal storage of soil water, and the annual water balance, *Adv. Water Resour.*, *17*(1–2), 19–24.

Nash, J., and J. Sutcliffe (1970), River flow forecasting through conceptual models part I—A discussion of principles, *J. Hydrol.*, *10*(3), 282–290.

Newsome, P., R. Wilde, and E. Willoughby (2008), Land resource information system spatial data layers, technical report, Landcare Res. NZ Ltd., Palmerston North, New Zealand, doi:10.7931/DL1V88.

NIWA (2015), *Climate Summaries*, New Zealand. [Available at http://www.niwa.co.nz/education-and-training/schools/resources/climate/summary.]

Ofir, M., and J. Kigel (1999), Photothermal control of the imposition of summer dormancy in Poabulbosa, a perennial grass geophyte, *Physiol. Plant.*, *105*(4), 633–640.

Orth, R., and S. I. Seneviratne (2014), Using soil moisture forecasts for sub-seasonal summer temperature predictions in Europe, *Clim. Dyn.*, *43*(12), 3403–3418.

Oudin, L., V. Andréassian, C. Perrin, and F. Anctil (2004), Locating the sources of low-pass behavior within rainfall-runoff models, *Water Resour. Res.*, *40*, W11101, doi:10.1029/2004WR003291.

Priestley, C. H. B., and R. J. Taylor (1972), On the assessment of surface heat flux and evaporation using large-scale parameters, *Mon. Weather Rev.*, *100*(2), 81–92.

Rodriguez-Iturbe, I. (2000), Ecohydrology: A hydrologic perspective of climate-soil-vegetation dynamies, *Water Resour. Res.*, *36*(1), 3–9.

Sampson, D., and H. Allen (1999), Regional influences of soil available water-holding capacity and climate, and leaf area index on simulated loblolly pine productivity, *For. Ecol. Manage.*, *124*(1), 1–12.

Schenk, H. J., and R. B. Jackson (2002), Rooting depths, lateral root spreads and below-ground/above-ground allometries of plants in water-limited ecosystems, *J. Ecol.*, *90*(3), 480–494.

Schymanski, S. J., M. Sivapalan, M. L. Roderick, J. Beringer, and L. B. Hutley (2008), An optimality-based model of the coupled soil moisture and root dynamics, *Hydrol. Earth Syst. Sci.*, *12*(3), 913–932.

Sivandran, G., and R. L. Bras (2013), Dynamic root distributions in ecohydrological modeling: A case study at Walnut Gulch Experimental Watershed, *Water Resour. Res.*, *49*, 3292–3305, doi:10.1002/wrcr.20245.

Tait, A., R. Henderson, R. Turner, and X. Zheng (2006), Thin plate smoothing spline interpolation of daily rainfall for New Zealand using a climatological rainfall surface, *Int. J. Climatol.*, *26*(14), 2097–2115.

Tait, A., J. Sturman, and M. Clark (2012), An assessment of the accuracy of interpolated daily rainfall for New Zealand, *J. Hydrol. N. Z.*, *51*(1), 25–44.

Troch, P. A., G. F. Martinez, V. R. N. Pauwels, M. Durcik, M. Sivapalan, C. Harman, P. D. Brooks, H. Gupta, and T. Huxman (2009), Climate and vegetation water use efficiency at catchment scales, *Hydrol. Processes*, *23*(16), 2409–2414.

Troch, P. A., T. Lahmers, A. Meira, R. Mukherjee, J. W. Pedersen, T. Roy, and R. Valds-Pineda (2015), Catchment coevolution: A useful framework for improving predictions of hydrological change?, *Water Resour. Res.*, *51*, 4903–4922, doi:10.1002/2015WR017032.

Tron, S., P. Perona, L. Gorla, M. Schwarz, F. Laio, and L. Ridolfi (2015), The signature of randomness in riparian plant root distributions, *Geophys. Res. Lett.*, *42*, 7098–7106, doi:10.1002/2015GL064857.

Vico, G., et al. (2015), Climatic, ecophysiological, and phenological controls on plant ecohydrological strategies in seasonally dry ecosystems, *Ecohydrology*, *8*(4), 660–681.

Wagener, T., N. McIntyre, M. J. Lees, H. S. Wheater, and H. V. Gupta (2003), Towards reduced uncertainty in conceptual rainfall-runoff modelling: Dynamic identifiability analysis, *Hydrol. Processes*, *17*(2), 455–476.

Wang-Erlandsson, L., et al. (2016), Global root zone storage capacity from satellite-based evaporation, *Hydrol. Earth Syst. Sci. Discuss.*, doi:10.5194/hess-2015-533, in review.

Webb, T., and A. Wilson (1995), *A Manual of Land Characteristics for Evaluation of Rural Land, Landcare Res. Sci. Ser.*, vol. 10, Manaaki Whenua Press, Lincoln, New Zealand.

Winsemius, H. C., H. H. G. Savenije, and W. G. M. Bastiaanssen (2008), Constraining model parameters on remotely sensed evaporation: Justification for distribution in ungauged basins?, *Hydrol. Earth Syst. Sci.*, *12*(6), 1403–1413.

Winsemius, H. C., B. Schaefli, A. Montanari, and H. H. G. Savenije (2009), On the calibration of hydrological models in ungauged basins: A framework for integrating hard and soft hydrological information, *Water Resour. Res.*, *45*, W12422, doi:10.1029/2009WR007706.

Woods, R., J. Hendrikx, R. Henderson, and A. Tait (2006), Estimating mean flow of New Zealand rivers, *J. Hydrol. N. Z.*, *45*(2), 95–110.

Zelikova, T. J., D. G. Williams, R. Hoenigman, D. M. Blumenthal, J. A. Morgan, and E. Pendall (2015), Seasonality of soil moisture mediates responses of ecosystem phenology to elevated CO_2 and warming in a semi-arid grassland, *J. Ecol.*, *103*, 1119–1130.

Zhang, L., W. R. Dawes, and G. R. Walker (2001), Response of mean annual evapotranspiration to vegetation changes at catchment scale, *Water Resour. Res.*, *37*(3), 701–708.